Accessing the Pion 3D Structure at US and China Electron-Ion Colliders

José Manuel Morgado Chávez,[1,*] Valerio Bertone,[2,†] Feliciano De Soto Borrero,[3,‡] Maxime Defurne,[2,§] Cédric Mezrag,[2,‖] Hervé Moutarde,[2,¶] José Rodríguez-Quintero,[1,**] and Jorge Segovia[3,††]

[1]*Department of Integrated Sciences and Center for Advanced Studies in Physics, Mathematics and Computation, University of Huelva, E-21071 Huelva, Spain*

[2]*Irfu, CEA, Université Paris-Saclay, 91191 Gif-sur-Yvette, France*

[3]*Departamento de Sistemas Físicos, Químicos y Naturales, Universidad Pablo de Olavide, E-41013 Sevilla, Spain*

(Received 29 October 2021; revised 22 December 2021; accepted 3 March 2022; published 17 May 2022)

We present the first systematic feasibility study of accessing generalized parton distributions of the pion at an electron-ion collider through deeply virtual Compton scattering. Relying on state-of-the-art models for pion GPDs, we show that quarks and gluons interfere destructively, modulating the expected event rate and maximizing it when parton content is generated via radiation from valence dressed quarks. Moreover, gluons are found to induce a sign inversion for the beam-spin asymmetry in every model studied, being a clear signal for pinning down the regime of gluon superiority.

DOI: 10.1103/PhysRevLett.128.202501

Introduction.—Due to its double role of being both a Goldstone boson of chiral symmetry breaking and a QCD bound state, the pion has been widely investigated since its discovery in 1947. Since the 1980s, many efforts were performed to extract experimental information about its internal structure, from its electromagnetic form factor (EFF) through pion-electron scattering [1] to its parton distribution functions (PDFs) through the Drell-Yan process [2–4]. The latter triggered a controversy on the PDF large-x behavior [5–9] enlightened by modern phenomenological and theoretical progresses [10], but also by simulation efforts [11–13]. Using the available pion sources, EFF measurements are limited to low-momentum transfer, precluding any test of perturbative QCD (pQCD) predictions [14,15]. However, exploiting the ideas of Sullivan [16], hinging on the premise of an interaction with the meson cloud of the proton, EFF data at significantly larger values of the momentum transfer between the incoming and outgoing pions have been obtained [17]. This same principle is being seriously considered both to improve the knowledge on the pion EFF and to extract the pion PDFs in the context of the forthcoming U.S. and Chinese electron ion colliders (EIC and EicC) [10,18,19]. The question has raised so much interest that the EIC Yellow Report [20] mentions the study of the 3D structure of the pion through the Sullivan process. The present paper is a quantitative assessment of the latter.

The 3D structure [21] of the pion can be accessed through generalized parton distributions (GPDs) [22–26]. Throughout the years, many models for pion GPDs have been developed [27–39], including in the crossed channel [40]. They rely on various physics assumptions and if feasible, deep virtual compton scattering (DVCS) [23] off the pion would provide key constraints on these models [41–43]. In this paper, relying on the implementation of the state-of-the-art models for the pion's GPDs, we compute the Sullivan amplitude at next-to-leading order (NLO), the minimal order required to treat the EIC kinematic region. We then evaluate the associated counting rate and assess the asymmetries, concluding that, provided that the one-pion exchange is the dominant process, DVCS off a virtual pion is measurable, triggering a clear signal for a glue-led regime: a sign inversion of the beam-spin asymmetry.

Modeling GPDs.—Among all available pion GPD models, we choose the one presented in Ref. [43], a kinematic completion of that featured in Ref. [39] owing to a long effort developed over the last decade [28–31,34,35]. This model is built on state-of-the-art continuum Schwinger method (CSM) investigations [44–50], which have provided the community with PDFs in agreement with the large-x behavior extracted from experimental data including soft-gluon (threshold) resummation [7,8] and are confirmed both in the quark and gluon sectors [51,52] by lattice QCD computations.

The leap from quark PDFs q_π to quark GPDs H_π^q is, however, made difficult because their dependences on x, the average momentum fraction of the active parton in the pion; ξ, half of the exchanged longitudinal momentum fraction; and t_π, the square of the total momentum transfer, are constrained by a set of properties [53,54]. To ensure that all properties are satisfied by construction, we turn to

the light-front wave function formalism [55] (see also Refs. [56–60] for details of the connection between CSM and light-front physics) supplemented by the so-called GPD covariant extension [34,35]. Our quark GPD in the DGLAP ($|x| \geq |\xi|$) region reads [43]

$$H_\pi^q(x,\xi,t_\pi) = \sqrt{q_\pi\left(\frac{x+\xi}{1+\xi}\right) q_\pi\left(\frac{x-\xi}{1-\xi}\right)}\,\Phi_\pi^q(x,\xi,t_\pi), \quad (1)$$

with

$$q_\pi(x) = \mathcal{N}_q x^2(1-x)^2[1+\gamma x(1-x)+\rho\sqrt{x(1-x)}], \quad (2)$$

$$\Phi_\pi^q(x,\xi,t_\pi) = \frac{1}{4}\frac{1}{1+\zeta^2}\left(3+\frac{1-2\zeta}{1+\zeta}\frac{\operatorname{arctanh}\left(\sqrt{\frac{\zeta}{1+\zeta}}\right)}{\sqrt{\frac{\zeta}{1+\zeta}}}\right), \quad (3)$$

where $\zeta = -t_\pi(1-x)^2/[4M^2(1-\xi^2)]$. It is modeled at a low reference scale $\mu_{\mathrm{Ref}} = 331$ MeV, defined in Refs. [49,50]. The PDF parameters obtained in Ref. [47] are $\mathcal{N}_q = 213$, $\gamma = 2.29$, and $\rho = -2.93$. The covariant extension provides us with the corresponding ERBL ($|x| \leq |\xi|$) region. Evolution equations from μ_{Ref} up to experimental scales are applied in the scheme introduced in Refs. [39,47,49], generating accordingly the gluon GPD. The latter yields a gluon PDF in excellent agreement with the one computed on the lattice [51,52]. This theoretical framework is reinforced by information coming from experimental extractions of EFF [17], fixing $M = 318$ MeV.

For comparison, we introduce a second pion GPD model based on phenomenology. Following Ref. [61], it is built on the basis of GRS PDFs [62], Radyushkin's double distribution *Ansatz* [63], and a "Reggeized" t_π parametrization [64]. It is labeled as the GRS model in the following.

In the case of the Sullivan process, one should consider a *transition* GPD between a virtual and a real pion. However, for low enough virtuality, it has been shown [65,66] that extrapolations from the standard GPD are possible. Therefore, virtuality effects are neglected in the chosen GPD model. This relies on a previous work on the pion EFF [65], indicating that neglecting virtualities does not undermine our conclusion on the feasibility of the measurement.

DVCS through the Sullivan process.—The DVCS amplitude is parametrized by a complex function $\mathcal{H}$ called the Compton form factor (CFF), a convolution of the pion GPDs and a hard kernel C computable within pQCD:

$$\mathcal{H}(\xi,t,Q^2) = \int_{-1}^{1}\frac{\mathrm{d}x}{2\xi}C\left(\frac{x}{\xi},\frac{Q^2}{\mu^2},\alpha_s\right)H(x,\xi,t,\mu^2). \quad (4)$$

At leading order (LO), C_{LO} selects only quark GPDs, while at NLO, an exchange of a gluon pair in the t channel is allowed [67–70]. Another competing process, called Bethe-Heitler (BH), leads to the same final state as DVCS, except that the real photon is emitted by either the incoming or outgoing lepton. As a consequence, the cross section for photon electroproduction off a pion $e\pi \to e\pi\gamma$ is the coherent sum of both processes' amplitudes:

$$\frac{d^5\sigma^{e\pi\to e\gamma\pi}(\lambda,\pm e)}{dy_\pi dx_B^\pi dt_\pi d\phi d\phi_e} = \frac{d^2\sigma_0}{dQ^2dx_B^\pi}\frac{|\mathcal{T}^{\mathrm{BH}}|^2+|\mathcal{T}^{DVCS}|^2 \mp \mathcal{I}(\lambda)}{e^6}, \quad (5)$$

$$\frac{d^2\sigma_0}{dQ^2dx_B^\pi} = \frac{\alpha_{\mathrm{QED}}^3 x_B^\pi y_\pi}{16\pi^2Q^2\sqrt{1+\epsilon^2}}, \quad (6)$$

with $\epsilon^2 = 4m_\pi^2(x_B^\pi)^2/Q^2$ (in the following we take $\epsilon = 0$) and $\mathcal{I}(\lambda) = \mathcal{I}_{\mathrm{unp}} + \lambda\mathcal{I}_{\mathrm{pol}}$. $\mathcal{T}^{\mathrm{BH/DVCS}}$ stands for the BH and DVCS amplitudes, respectively, and $\mathcal{I}_{\mathrm{unp/pol}}$ stands for the unpolarized and polarized interference terms. λ is the electron helicity, $-e$ its charge, α_{QED} the electromagnetic coupling, ϕ_e the azimuthal angle of the scattered lepton, m_π the mass of the pion, and ϕ the angle between the leptonic and hadronic planes, defined according to the Trento convention [71]. $\mathcal{T}^{DVCS}$ depends on $|\mathcal{H}|^2$, while $\mathcal{I}_{\mathrm{unp/pol}}$ gives access to $\Re(\mathcal{H})$ and $\Im(\mathcal{H})$ independently. In order to compute CFFs from the GPD model introduced above, we took advantage of PARTONS [72], where the formulas of Refs. [69,70,73] are implemented, together with APFEL++ [74–76], providing us with a LO evolution routine for GPDs.

Two additional variables are required to characterize the virtual pion in the initial state: $x_\pi = (p_\pi\cdot l/p\cdot l)$ being the fraction of the proton energy carried by the virtual pion in the ep center-of-mass frame and $t = p_\pi^2$. Following Ref. [61], the cross section of the Sullivan process (see Fig. 1) reads

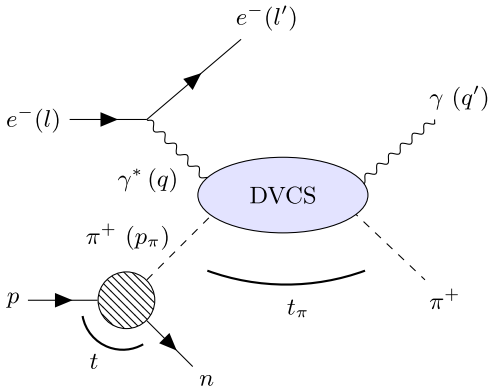

FIG. 1. DVCS off a virtual pion through the Sullivan process. Kinematic variables: $Q^2 = -q^2$, $y = (p\cdot q/p\cdot l)$, $y_\pi = (p_\pi\cdot q/p_\pi\cdot l)$, and $x_B^\pi = (Q^2/2p_\pi\cdot q)$.

$$\frac{d^8\sigma^{\mathrm{Sul}}(\lambda,\pm e)}{dydQ^2dt_\pi d\phi d\phi_e dt dx_\pi d\phi_n} = x_\pi \frac{g^2_{\pi NN}}{16\pi^3} F(t;\Lambda^2)^2 \frac{-t}{(m_\pi^2-t)^2} \left| J^{Q^2}_{x_B^\pi} \right| \frac{d^5\sigma^{e\pi\to e\gamma\pi}(\lambda,\pm e)}{dy_\pi dx_B^\pi dt_\pi d\phi d\phi_e}, \tag{7}$$

with $J^{Q^2}_{x_B^\pi}$ being the Jacobian between Q^2 and x_B^π, ϕ_n as the azimuthal angle of the spectator neutron, and $g_{\pi NN} = 13.05$ being the pion-nucleon coupling constant. The factor $F(t;\Lambda)$ with $\Lambda = 800$ MeV is introduced to reduce the pion-nucleon vertex as $|t|$ increases [61].

In order to ensure a proper interpretation of the event as a Sullivan DVCS process, the pion virtuality $|t|$ must be small enough and will be taken such that $|t| \leq |t|_{\max} = 0.6$ GeV^2 and $s_\pi = (p_\pi + q)^2 > s_\pi^{\min} = 4$ GeV^2 [61]. In addition, to reduce the contribution from nucleon resonances N^* through the process $ep \to eN^*\gamma \to en\pi\gamma$, the invariant mass of the $n\pi$ system is required to be larger than 2 GeV. For the sake of completeness, let us mention that there are also contributions which cannot be easily restricted by cutting on kinematic variables. For instance, virtual ρ's may contribute through $\gamma^*\rho \to \gamma\pi$ and can only be assessed with a model of transition form factors and GPDs. We neglect them in the present study.

Evaluation of observables.—Both EIC and EicC facilities will deliver highly polarized lepton and hadron beams. Their characteristics can be found in Refs. [19,20], and the coverage they offer is illustrated in Fig. 2.

Regarding the EIC's design [20], a central barrel detector with two end caps, sitting in a 3 T solenoidal magnetic field, will be in charge of spotting the scattered lepton, the photon, and the recoil pion with pseudorapidity between −4 and 4. A far-forward spectrometer will detect the recoil pion with a polar angle between 6 and 20 mrad. A zero-degree calorimeter will detect the neutron with polar angles from 0 to 5.5 mrad. EicC is analogously designed, with

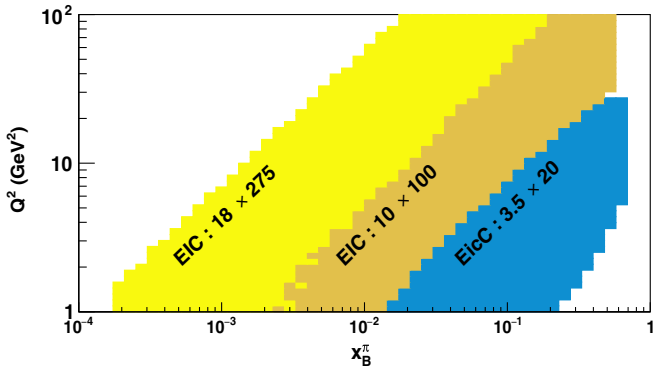

FIG. 2. Phase space considered in the present study: facilities and configurations (electron × proton beam energies in GeV) contributing the most to the statistics in the colored areas are specified.

central and forward detectors [19]. However, as it is still at a conceptual stage, key parameters for our study are not provided, such as the acceptance for the neutron. Hence, we assume ideal geometry for the EicC spectator neutron tagger.

To guarantee exclusivity, a reliable detection and identification of the electron, the photon, and the neutron is assumed. Momentum conservation will be required, and therefore pion identification is not considered to be mandatory.

The number of events is then estimated by Monte Carlo simulation. From Eq. (7), five kinematic variables and three angles are necessary to fully determine the final state. They are all uniformly generated. After cuts guaranteeing the validity of the Sullivan process [61], the number of expected events $\mathcal{N}$ is obtained by

$$\mathcal{N} = \mathcal{L} \sum_{i\in\Phi} \frac{d^8\sigma^i(\lambda,\pm e)}{dydQ^2dt_\pi d\phi d\phi_e dt dx_\pi d\phi_n} \times \frac{\Delta\Phi^i}{N_{\mathrm{gen}}}, \tag{8}$$

where Φ is the phase space of events passing kinematic cuts with all final-state particles detected, $\Delta\Phi^i$ is the hypervolume in which the kinematic variables have been generated for event i, N_{gen} is the number of generated events, and $\mathcal{L}$ is the integrated luminosity over a year.

In the CSM approach, two scenarios are compared: CFFs computed at NLO with ($\mathcal{H}^{\mathrm{CSM}}$) and without ($\mathcal{H}^{\mathrm{CSM}}_{0g}$) the contribution of gluon GPDs. Full NLO results from the GRS model are also evaluated. From Fig. 3, presenting expected count rates and beam-spin asymmetries (BSA) for $x_B^\pi \in [10^{-3}; 10^{-2}]$ and four different Q^2 bins, several conclusions can be drawn.

Event rates: First, both CSM and GRS computations predict event rates clearly not compatible with solely a BH signal, highlighting the possibility of accessing DVCS on a pion target at future electron ion colliders. Their behavior is consistent, suggesting both thousands of events a year and an important increase of the event rate at low Q^2.

However, in the lower bin in Q^2, the central value of the predictions regarding the strength of the signal significantly differs between the two models, although the results still remain fully consistent within the uncertainties. The difference is much larger than the expected experimental uncertainties, highlighting the *major* discriminating power of the DVCS cross section measurements. Note again that the two models' predictions can be reconciled if one considers a ±10% uncertainty in the original scale, stressing the sensibility of the model at very low Q^2, which nonetheless decreases quickly as Q^2 rises.

To understand this behavior, we provide computations with ($\mathcal{H}^{\mathrm{CSM}}$) and without ($\mathcal{H}^{\mathrm{CSM}}_{0g}$) gluon contributions for the CSM model. Thus, we emphasize the major contribution of gluons to the process amplitude. Since quark and gluon contributions to CFFs show opposite signs, "destructive interferences" reduce the counting rates for

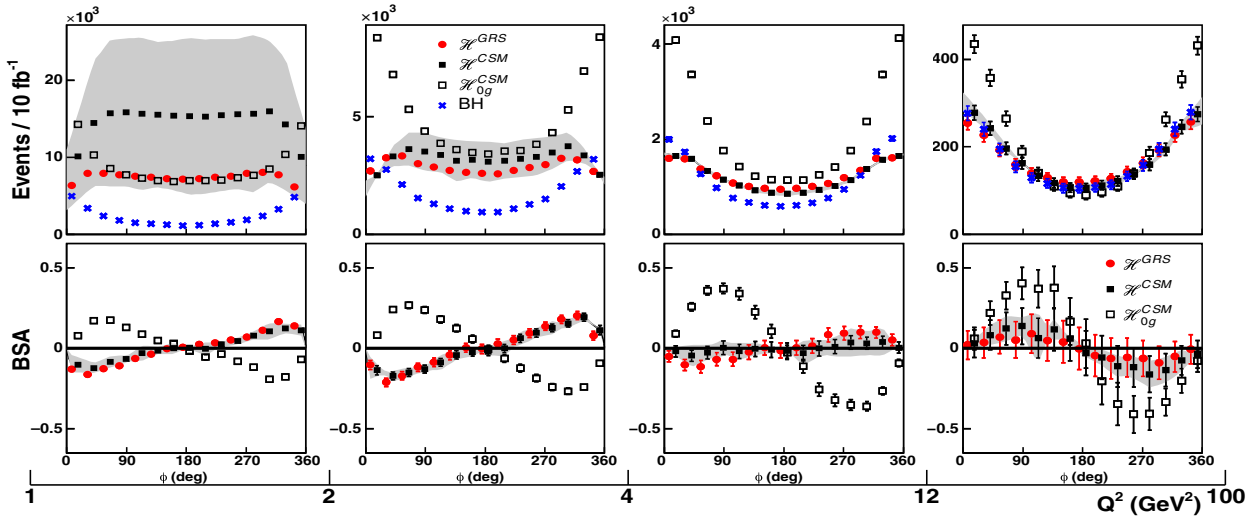

FIG. 3. Number of DVCS events (upper chart) and expected beam-spin asymmetries (lower chart) as functions of Q^2 for $x_B^\pi \in [10^{-3}; 10^{-2}]$. Black squares represent the full NLO calculation in the model of Ref. [43], while empty squares show the NLO evaluation without taking the gluon contribution into account. Red circles display NLO results from the GRS model, and blue crosses denote the BH event rate. The shaded gray area shows the evolution-induced uncertainty.

$2 < Q^2 < 12$ GeV^2. Below, α_s is large enough for the gluon contribution to dominate the process, strongly increasing the counting rate. The large uncertainty in this region can be related to gluon GPDs.

In summary, from the analysis of the upper panels in Fig. 3, two general features can be highlighted: (i) gluon content plays a major role driving the response of pions subjected to deeply virtual Compton scattering, and (ii) gluon and quark distributions "interfere," modulating the expected count rates. This picture explains the discrepancy between CSM and GRS predictions: following the CSM approach, in the $Q^2 < 2$ GeV^2 domain, the gluon contribution to the CFFs largely dominates the quark one; for the GRS model, gluon contributions are still stronger than quark contributions, but comparatively weaker than in the CSM case.

Beam-spin asymmetries: We now turn to the study of BSAs, whose amplitudes' sign directly depends on that of the imaginary part of the CFFs. We note that being a ratio, BSAs are much more resilient to the uncertainties previously highlighted (but also carry less discriminating power between models). As shown by the lower panels in Fig. 3, every model explored here predicts compatible results regarding a sign inversion for the beam-spin asymmetry in the low-Q^2 regime. Such a sign change highlights that the gluon contribution to the imaginary part of the CFF is larger (in absolute value) than the quark one. Pinning down a zero crossing would emphasize the transition between a quark- and a gluon-driven understanding of DVCS. Both models predict that a sign change in the BSA will take place at EIC kinematics.

Valence region (EicC): Remarkably, the gluon contribution remains sizeable in the valence region accessible through EicC (see Fig. 2) with high statistical accuracy, as shown in Fig. 4. At NLO and without the gluon contribution in the valence region, the BSA's amplitude does not change much as a function of Q^2 and reaches about 0.2. Contrarily, when the gluon GPD is considered, it almost vanishes at low Q^2, then rapidly increases with Q^2 but remains smaller by a factor of 2 compared to the gluonless case. The important role of gluons, even for EicC kinematics close to the valence region, was to be expected both from theoretical studies on the nucleon (see Ref. [70]) and from experimental studies [77] close to or within the valence region.

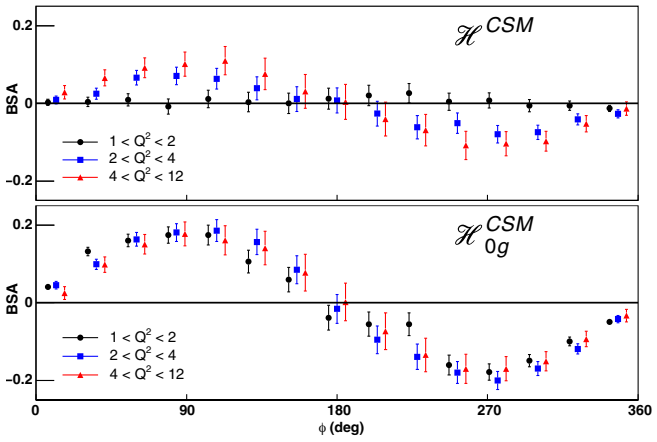

FIG. 4. Expected beam-spin asymmetries as functions of ϕ with $\mathcal{H}^{\mathrm{CSM}}$ (top) and $\mathcal{H}^{\mathrm{CSM}}_{0g}$ (bottom) from EicC for $x_B^\pi \in [0.1; 0.5]$ and three different Q^2 bins: black circles for Q^2 between 1 and 2 GeV^2, blue squares between 2 and 4 GeV^2, and red triangles between 4 and 12 GeV^2.

Conclusions.—We have studied the possibility to probe experimentally the pion's 3D structure through the Sullivan process. Using a state-of-the-art model based on continuum Schwinger methods yielding predictions in agreement with lattice QCD calculations for the gluon PDF [51,52] and extractions of DVCS amplitudes through dispersion relations with one subtraction constant [78], we obtained for one year of integrated luminosity at EIC and EicC a significant number of events. This shows that DVCS off a virtual pion will be measurable, provided that the one-pion exchange is the dominant process. Through the present analysis on the Q^2/x_B^π dependence, it is shown that even if gluons were overestimated by their generation through the splitting of dressed valence quarks, optimism about accessing the pion's 3D structure at forthcoming electron-ion colliders may be raised in the low-x region, a prediction which remains compatible with phenomenological analyses. In addition, the expected statistics should be high enough to also study the t dependence of the DVCS amplitude. We also highlighted a signal for gluon dominance of the DVCS cross section—namely, that the beam-spin asymmetry undergoes a sign inversion induced by the gluon contribution to the DVCS amplitude. Remarkably, this behavior has been verified to show up through different modeling approaches and within the expected evolution-induced uncertainty. The wide kinematic coverage coupled with the high luminosity of EIC and EicC should allow us to see this effect. Since the role of the two-gluon exchange in the t channel becomes dominant, next-to-next-to-leading-order corrections to the DVCS kernel [79] are certainly desirable, and may confirm the behavior highlighted here at NLO.

We would like to thank P. Barry, H. Dutrieux, T. Meisgny, B. Pire, K. Raya, C. D. Roberts, D. Sokhan, Q.-T. Song, P. Sznajder, and J. Wagner for interesting discussions and stimulating comments. This work is supported by the University of Huelva under Grant No. EPIT-2020 (J. M. M. C.). F. S., J. R. Q., and J. S. acknowledge support from Ministerio de Ciencia e Innovación (Spain) under Grant No. PID2019–107844 GB-C22 and Junta de Andalucía, under the 2014-2020 FEDER Contracts No. UHU-1264517, No. P18-1321FR-5057 and No. PAIDI FQM-370. This project was supported by the European Union's Horizon 2020 research and innovation program under Grant Agreement No. 824093. This work is supported in part in the framework of the GLUODYNAMICS project funded by the "P2IO LabEx" (No. ANR-10-LABX-0038) in the framework "Investissements d'Avenir" (No. ANR-11-IDEX-0003-01) managed by the Agence Nationale de la Recherche (ANR), France.

[*]josemanuel.morgado@dci.uhu.es
[†]valerio.bertone@cea.fr
[‡]fcsotbor@upo.es
[§]maxime.defurne@cea.fr
[‖]cedric.mezrag@cea.fr
[¶]herve.moutarde@cea.fr
[**]jose.rodriguez@dfaie.uhu.es
[††]jsegovia@upo.es

[1] S. Amendolia *et al.* (NA7 Collaboration), A measurement of the space-like pion electromagnetic form-factor, Nucl. Phys. **B277**, 168 (1986).
[2] J. S. Conway, C. E. Adolphsen, J. P. Alexander, K. J. Anderson, J. E. Heinrich, J. E. Pilcher, A. Possoz, E. I. Rosenberg, C. Biino, J. F. Greenhalgh, W. C. Louis, K. T. McDonald, S. Palestini, F. C. Shoemaker, and A. J. S. Smith, Experimental study of muon pairs produced by 252-GeV pions on tungsten, Phys. Rev. D **39**, 92 (1989).
[3] P. Bordalo *et al.* (NA10 Collaboration), Observation of a nuclear dependence of the transverse momentum distribution of massive muon pairs produced in hadronic collisions, Phys. Lett. B **193**, 373 (1987).
[4] B. Betev *et al.* (NA10 Collaboration), Differential cross-section of high mass muon pairs produced by a 194-GeV/$c\pi^-$ beam on a tungsten target, Z. Phys. C **28**, 9 (1985).
[5] P. C. Barry, N. Sato, W. Melnitchouk, and C.-R. Ji, First Monte Carlo Global QCD Analysis of Pion Parton Distributions, Phys. Rev. Lett. **121**, 152001 (2018).
[6] I. Novikov, H. Abdolmaleki, D. Britzger, A. Cooper-Sarkar, F. Giuli, A. Glazov, A. Kusina, A. Luszczak, F. Olness, P. Starovoitov, M. Sutton, and O. Zenaiev, Parton distribution functions of the charged pion within the xFitter framework, Phys. Rev. D **102**, 014040 (2020).
[7] P. C. Barry, C.-R. Ji, N. Sato, and W. Melnitchouk, Global QCD Analysis of Pion Parton Distributions with Threshold Resummation, Phys. Rev. Lett. **127**, 232001 (2021).
[8] M. Aicher, A. Schafer, and W. Vogelsang, Soft-Gluon Resummation and the Valence Parton Distribution Function of the Pion, Phys. Rev. Lett. **105**, 252003 (2010).
[9] C. Han, G. Xie, R. Wang, and X. Chen, An analysis of parton distribution functions of the pion and the kaon with the maximum entropy input, Eur. Phys. J. C **81**, 302 (2021).
[10] J. Arrington *et al.*, Revealing the structure of light pseudoscalar mesons at the electron-ion collider, J. Phys. G **48**, 075106 (2021).
[11] J.-H. Zhang, J.-W. Chen, L. Jin, H.-W. Lin, A. Schäfer, and Y. Zhao, First direct lattice-QCD calculation of the x-dependence of the pion parton distribution function, Phys. Rev. D **100**, 034505 (2019).
[12] B. Joó, J. Karpie, K. Orginos, A. V. Radyushkin, D. G. Richards, R. S. Sufian, and S. Zafeiropoulos, Pion valence structure from Ioffe-time parton pseudodistribution functions, Phys. Rev. D **100**, 114512 (2019).
[13] X. Gao, L. Jin, C. Kallidonis, N. Karthik, S. Mukherjee, P. Petreczky, C. Shugert, S. Syritsyn, and Y. Zhao, Valence parton distribution of the pion from lattice QCD: Approaching the continuum limit, Phys. Rev. D **102**, 094513 (2020).
[14] A. Efremov and A. Radyushkin, Factorization and asymptotical behavior of pion form-factor in QCD, Phys. Lett. **94B**, 245 (1980).
[15] G. P. Lepage and S. J. Brodsky, Exclusive processes in perturbative quantum chromodynamics, Phys. Rev. D **22**, 2157 (1980).

[16] J. D. Sullivan, One pion exchange and deep inelastic electron-nucleon scattering, Phys. Rev. D **5**, 1732 (1972).

[17] G. M. Huber *et al.* (Jefferson Lab), Charged pion form-factor between $Q^2 = 0.60$ GeV^2 and 2.45 GeV^2: II. Determination of, and results for, the pion form-factor, Phys. Rev. C **78**, 045203 (2008).

[18] A. C. Aguilar *et al.*, Pion and kaon structure at the electron-ion collider, Eur. Phys. J. A **55**, 190 (2019).

[19] D. P. Anderle *et al.*, Electron-ion collider in China, Front. Phys. (Beijing) **16**, 64701 (2021).

[20] R. Abdul-Khalek *et al.*, Science requirements and detector concepts for the electron-ion collider: EIC Yellow report, arXiv:2103.05419.

[21] M. Burkardt, Impact parameter dependent parton distributions and off forward parton distributions for $\zeta \to 0$, Phys. Rev. D **62**, 071503 (2000); **66**, 119903(E) (2002).

[22] D. Müeller, D. Robaschik, B. Geyer, F. M. Dittes, and J. Hořejši, Wave functions, evolution equations and evolution kernels from light ray operators of QCD, Fortschr. Phys. **42**, 101 (1994).

[23] X. Ji, Deeply virtual Compton scattering, Phys. Rev. D **55**, 7114 (1997).

[24] X. Ji, Gauge-Invariant Decomposition of Nucleon Spin, Phys. Rev. Lett. **78**, 610 (1997).

[25] A. Radyushkin, Asymmetric gluon distributions and hard diffractive electroproduction, Phys. Lett. B **385**, 333 (1996).

[26] A. V. Radyushkin, Nonforward parton distributions, Phys. Rev. D **56**, 5524 (1997).

[27] T. Frederico, E. Pace, B. Pasquini, and G. Salme, Pion generalized parton distributions with covariant and light-front constituent quark models, Phys. Rev. D **80**, 054021 (2009).

[28] C. Mezrag, H. Moutarde, and F. Sabatié, Test of two new parameterizations of the generalized parton distribution H, Phys. Rev. D **88**, 014001 (2013).

[29] C. Mezrag, H. Moutarde, J. Rodríguez-Quintero, and F. Sabatié, Towards a pion generalized parton distribution model from Dyson-Schwinger equations, arXiv:1406.7425.

[30] C. Mezrag, L. Chang, H. Moutarde, C. D. Roberts, J. Rodríguez-Quintero, F. Sabatié, and S. M. Schmidt, Sketching the pion's valence-quark generalised parton distribution, Phys. Lett. B **741**, 190 (2015).

[31] C. Mezrag, H. Moutarde, and J. Rodriguez-Quintero, From Bethe-Salpeter wave functions to generalised parton distributions, Few Body Syst. **57**, 729 (2016).

[32] C. Fanelli, E. Pace, G. Romanelli, G. Salme, and M. Salmistraro, Pion generalized parton distributions within a fully covariant constituent quark model, Eur. Phys. J. C **76**, 253 (2016).

[33] M. Rinaldi, GPDs at non-zero skewness in ADS/QCD model, Phys. Lett. B **771**, 563 (2017).

[34] N. Chouika, C. Mezrag, H. Moutarde, and J. Rodríguez-Quintero, Covariant extension of the GPD overlap representation at low Fock states, Eur. Phys. J. C **77**, 906 (2017).

[35] N. Chouika, C. Mezrag, H. Moutarde, and J. Rodríguez-Quintero, A Nakanishi-based model illustrating the covariant extension of the pion GPD overlap representation and its ambiguities, Phys. Lett. B **780**, 287 (2018).

[36] G. F. de Teramond, T. Liu, R. S. Sufian, H. G. Dosch, S. J. Brodsky, and A. Deur (HLFHS), Universality of Generalized Parton Distributions in Light-Front Holographic QCD, Phys. Rev. Lett. **120**, 182001 (2018).

[37] C. Shi, K. Bednar, I. C. Cloët, and A. Freese, Spatial and momentum imaging of the pion and kaon, Phys. Rev. D **101**, 074014 (2020).

[38] J.-L. Zhang, Z.-F. Cui, J. Ping, and C. D. Roberts, Contact interaction analysis of pion GTMDs, Eur. Phys. J. C **81**, 6 (2021).

[39] K. Raya, Z.-F. Cui, L. Chang, J. M. Morgado, C. D. Roberts, and J. Rodriguez-Quintero, Revealing pion and kaon structure via generalised parton distributions, Chin. Phys. C **46**, 013105 (2022).

[40] S. Kumano, Q.-T. Song, and O. V. Teryaev, Hadron tomography by generalized distribution amplitudes in pion-pair production process $\gamma^*\gamma \to \pi^0\pi^0$ and gravitational form factors for pion, Phys. Rev. D **97**, 014020 (2018).

[41] V. Bertone, H. Dutrieux, C. Mezrag, H. Moutarde, and P. Sznajder, Deconvolution problem of deeply virtual Compton scattering, Phys. Rev. D **103**, 114019 (2021).

[42] V. Bertone, H. Dutrieux, C. Mezrag, H. Moutarde, and P. Sznajder, Shadow generalized parton distributions: a practical approach to the deconvolution problem of DVCS, in *28th International Workshop on Deep Inelastic Scattering and Related Subjects* (2021), arXiv:2107.11312.

[43] J. M. M. Chavez, V. Bertone, F. D. S. Borrero, M. Defurne, C. Mezrag, H. Moutarde, J. Rodríguez-Quintero, and J. Segovia, companion paper, Pion generalized parton distributions: A path toward phenomenology, Phys. Rev. D **105**, 094012 (2022).

[44] D. Binosi, L. Chang, J. Papavassiliou, S.-X. Qin, and C. D. Roberts, Symmetry preserving truncations of the gap and Bethe-Salpeter equations, Phys. Rev. D **93**, 096010 (2016).

[45] S.-X. Qin, A systematic approach to sketch Bethe-Salpeter equation, EPJ Web Conf. **113**, 05024 (2016).

[46] S.-X. Qin and C. D. Roberts, Resolving the Bethe-Salpeter Kernel, Chin. Phys. Lett. **38**, 071201 (2021).

[47] M. Ding, K. Raya, D. Binosi, L. Chang, C. D. Roberts, and S. M. Schmidt, Symmetry, symmetry breaking, and pion parton distributions, Phys. Rev. D **101**, 054014 (2020).

[48] M. Ding, K. Raya, D. Binosi, L. Chang, C. D. Roberts, and S. M. Schmidt, Drawing insights from pion parton distributions, Chin. Phys. C **44**, 031002 (2020).

[49] Z.-F. Cui, M. Ding, F. Gao, K. Raya, D. Binosi, L. Chang, C. D. Roberts, J. Rodríguez-Quintero, and S. M. Schmidt, Kaon and pion parton distributions, Eur. Phys. J. C **80**, 1064 (2020).

[50] Z.-F. Cui, M. Ding, F. Gao, K. Raya, D. Binosi, L. Chang, C. D. Roberts, J. Rodríguez-Quintero, and S. M. Schmidt, Higgs modulation of emergent mass as revealed in kaon and pion parton distributions, Eur. Phys. J. A **57**, 5 (2021).

[51] Z. Fan and H.-W. Lin, Gluon parton distribution of the pion from lattice QCD, Phys. Lett. B **823**, 136778 (2021).

[52] L. Chang and C. D. Roberts, Regarding the distribution of glue in the pion, Chin. Phys. Lett. **38**, 081101 (2021).

[53] M. Diehl, Generalized parton distributions, Phys. Rep. **388**, 41 (2003).

[54] A. Belitsky and A. Radyushkin, Unraveling hadron structure with generalized parton distributions, Phys. Rep. **418**, 1 (2005).

[55] M. Diehl, T. Feldmann, R. Jakob, and P. Kroll, The overlap representation of skewed quark and gluon distributions, Nucl. Phys. **B596**, 33 (2001).
[56] T. Frederico, G. Salme, and M. Viviani, Two-body scattering states in Minkowski space and the Nakanishi integral representation onto the null plane, Phys. Rev. D **85**, 036009 (2012).
[57] L. Chang, I. C. Cloet, J. J. Cobos-Martinez, C. D. Roberts, S. M. Schmidt, and P. C. Tandy, Imaging Dynamical Chiral Symmetry Breaking: Pion Wave Function on the Light Front, Phys. Rev. Lett. **110**, 132001 (2013).
[58] J. Carbonell, T. Frederico, and V. A. Karmanov, Bound state equation for the Nakanishi weight function, Phys. Lett. B **769**, 418 (2017).
[59] G. Salmé, W. de Paula, T. Frederico, and M. Viviani, Two-Fermion Bethe-Salpeter equation in Minkowski space: The Nakanishi way, Few Body Syst. **58**, 118 (2017).
[60] C. Mezrag and G. Salmé, Fermion and photon gap-equations in Minkowski space within the Nakanishi integral representation method, Eur. Phys. J. C **81**, 34 (2021).
[61] D. Amrath, M. Diehl, and J.-P. Lansberg, Deeply virtual Compton scattering on a virtual pion target, Eur. Phys. J. C **58**, 179 (2008).
[62] M. Gluck, E. Reya, and I. Schienbein, Pionic parton distributions revisited, Eur. Phys. J. C **10**, 313 (1999).
[63] I. V. Musatov and A. V. Radyushkin, Evolution and models for skewed parton distributions, Phys. Rev. D **61**, 074027 (2000).
[64] M. Diehl, T. Feldmann, R. Jakob, and P. Kroll, Generalized parton distributions from nucleon form-factor data, Eur. Phys. J. C **39**, 1 (2005).
[65] S.-X. Qin, C. Chen, C. Mezrag, and C. D. Roberts, Off-shell persistence of composite pions and kaons, Phys. Rev. C **97**, 015203 (2018).
[66] R. J. Perry, A. Kızılersü, and A. W. Thomas, Model dependence of the pion form factor extracted from pion electroproduction, Phys. Rev. C **100**, 025206 (2019).
[67] X. Ji and J. Osborne, One loop QCD corrections to deeply virtual Compton scattering: The Parton helicity independent case, Phys. Rev. D **57**, R1337 (1998).
[68] A. V. Belitsky, D. Mueller, L. Niedermeier, and A. Schafer, Deeply virtual Compton scattering in next-to-leading order, Phys. Lett. B **474**, 163 (2000).
[69] B. Pire, L. Szymanowski, and J. Wagner, NLO corrections to timelike, spacelike and double deeply virtual Compton scattering, Phys. Rev. D **83**, 034009 (2011).
[70] H. Moutarde, B. Pire, F. Sabatie, L. Szymanowski, and J. Wagner, On timelike and spacelike deeply virtual Compton scattering at next to leading order, Phys. Rev. D **87**, 054029 (2013).
[71] A. Bacchetta, U. D'Alesio, M. Diehl, and C. A. Miller, Single-spin asymmetries: The Trento conventions, Phys. Rev. D **70**, 117504 (2004).
[72] B. Berthou, D. Binosi, N. Chouika, L. Colaneri, M. Guidal, C. Mezrag, H. Moutarde, J. Rodríguez-Quintero, F. Sabatié, P. Sznajder, and J. Wagner, PARTONS: Partonic tomography of nucleon software. A computing framework for the phenomenology of Generalized Parton Distributions, Eur. Phys. J. C **78**, 478 (2018).
[73] A. V. Belitsky and D. Müeller, Refined analysis of photon leptoproduction off spinless target, Phys. Rev. D **79**, 014017 (2009).
[74] V. Bertone, S. Carrazza, and J. Rojo, APFEL: A PDF evolution library with QED corrections, Comput. Phys. Commun. **185**, 1647 (2014).
[75] V. Bertone, APFEL++: A new PDF evolution library in C++, Proc. Sci., DIS2017 (**2018**) 201 [arXiv:1708.00911].
[76] V. Bertone and Collaborators, Revisiting evolution equations for generalised parton distributions (to be published).
[77] M. Defurne *et al.*, A glimpse of gluons through deeply virtual compton scattering on the proton, Nat. Commun. **8**, 1408 (2017).
[78] M. Diehl and D. Y. Ivanov, Dispersion representations for hard exclusive processes: Beyond the Born approximation, Eur. Phys. J. C **52**, 919 (2007).
[79] V. M. Braun, A. N. Manashov, S. Moch, and J. Schoenleber, Two-loop coefficient function for DVCS: Vector contributions, J. High Energy Phys. 09 (2020) 117.